AIChE WILEY InterScience DISCOVER SOMETHING GREAT

Using Feasible Regions to Design and Optimize Reactive Distillation Columns with Ideal VLE

Warren R. Hoffmaster and Steinar Hauan
Dept. of Chemical Engineering, Carnegie Mellon University, Pittsburgh, PA 15213

DOI 10.1002/aic.10765
Published online January 6, 2006 in Wiley InterScience (www.interscience.wiley.com).

The design and optimization of reactive distillation columns using feasibility analysis is addressed. Based on the feasible regions identified in previous work, we present two examples to illustrate the benefits of having feasibility information when locating design alternatives for systems with ideal vapor–liquid equilibrium. The examples include a reactive column for the metathesis of 2-pentene and a multifeed reactive column with a constant volatility mixture. In the first example, we use the feasible regions to initialize an optimization-based design strategy. For the second example, we characterize the feasible regions to determine feasible placement strategies for side streams and reactive stages. The design insights gained from feasibility analysis are highlighted for each example.
 AIChE J, 52: 1744–1753, 2006
Keywords: reactive distillation design, feasibility analysis, feasible regions

Introduction

Modeling techniques for reactive distillation columns are well developed, as evidenced by recent reviews.[1,2] These models, which are extensions to nonreactive methods, have seen widespread use for designing reactive distillation columns. The available design techniques can be classified into four categories: simulation, iterative design, feasibility analysis, and optimization. The simulation methods[3,4] rely on specified inputs and operating parameters to determine the resulting outputs. Iterative techniques[5,6] use a selected set of inputs, outputs, and operating parameters. Then, the remaining parameters are varied to find a feasible set that achieves the given product specifications. There are also methods that use feasibility analysis[7-9] to capture all possible design alternatives. In addition, optimization has been used to determine the most economical reactive distillation design alternatives.[10,11]

Process simulators are difficult to use when dealing with problems that have unknown design parameters (such as number of stages) and specified output constraints (such as product purities). Numerous parametric studies must be performed in the simulator to understand the conditions that make a design feasible. The iterative design and feasibility analysis methods provide geometric insights useful in determining full column feasibility but are limited to single-feed columns with two products. Iterative and feasible region approaches typically restrict how the reaction is distributed throughout a column. They either assume reaction equilibrium or a constant amount of reactive liquid holdup from stage to stage. This can result in suboptimal designs. When formulated properly, optimization methods are able to find good designs with arbitrary reaction distribution policies and multiple side streams. Subsequent analysis of a collection of these locally optimal solutions may be analyzed to reveal more general traits of why particular designs are more economical than others.

Recently, we have developed a feasibility analysis technique that applies to distillation columns with kinetically controlled reactions and multiple side streams.[12] Our approach accounts for an arbitrary reaction distribution policy. In this method, we decompose full columns into sections and capture sectional profiles for the full range of operating parameters in what is known as a feasible region. The regions are represented in composition space and can be used to graphically test for full column feasibility. Although the feasible region techniques apply to both ideal and nonideal systems, this article will specifically address designs for mixtures with ideal vapor–liquid equilibrium (VLE). The report applies the feasibility analysis technique to two examples. We will demonstrate how

Correspondence concerning this article should be addressed to S. Hauan at hauan@cmu.edu.

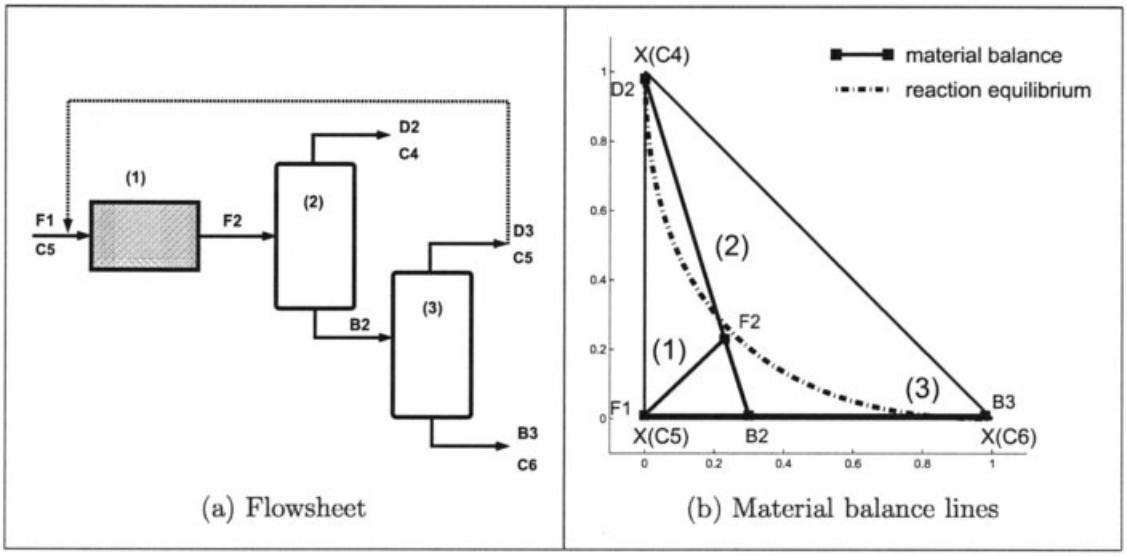

Figure 1. Olefin metathesis design with sequential unit operations.

to use feasible regions to initialize an optimization approach for reactive distillation design. We will also illustrate how to use feasible regions to properly distribute reaction and side streams in a column without having to carry out significant iterations. The main objective herein is to show how our feasibility analysis approach complements both iterative and optimization-based design methods for reactive distillation.

Examples

We present two examples to illustrate how to use feasible regions to design complex columns with chemical reactions. Each example highlights a different aspect of complex column design and shows the benefits of feasibility analysis. The goal of these examples is to illustrate the range of design capabilities and insights resulting from feasible region identification. The first example investigates an olefin metathesis reactive distillation column. This example uses feasible regions to initialize an optimization-based design strategy. A multifeed reactive column with a constant volatility mixture is the focus of the second example, which shows how to characterize the feasible regions to determine placement strategies for all side feeds and reactive stages without the need for extensive iterative techniques.

Example 1: Olefin metathesis

Metathesis reactions are important for rebalancing the light olefins obtained from steam cracking or catalytic cracking. Recent literature[6,8,11] and patents[13,14] investigate the use of reactive distillation for olefin metathesis. We will study the metathesis of 2-pentene to form 2-butene and 3-hexene shown in the following equation:

$$2C_5H_{10} \rightleftharpoons C_4H_8 + C_6H_{12} \quad (1)$$

The physical properties and reaction kinetics are taken from Okasinski and Doherty.[6] The reaction occurs in the liquid phase with a negligible heat of reaction. We assume the mixture has ideal VLE behavior at atmospheric pressure. All residue curves for this system begin at butene (277 K), travel toward pentene (310 K), and terminate at hexene (340 K). We will investigate design alternatives for both sequential and simultaneous reaction and separation. Specifically, we seek out alternatives that convert a pure pentene feed into butene and hexene products with at least 98 mol % purity.

Alternative 1: Sequential unit operations

One design alternative uses an equilibrium reactor followed by a pair of distillation columns as shown in Figure 1a. The material balance lines for this configuration are identified in Figure 1b. Pure pentene (F1) is fed to the reactor with output (F2) approaching reaction equilibrium. This ternary mixture feeds a direct split column. Nearly pure butene (D2) is recovered overhead, and a mixture of pentene and hexene exits as the bottoms product (B2). The binary mixture then enters another column to separate pentene (D3 = F1) from hexene (B3). The unreacted pentene may be recycled back to the reactor. This design achieves only 50% per-pass conversion of pentene because of equilibrium limitations. As a result of the poor conversion, significant energy is required to separate the unreacted pentene from the two products. No significant benefit can be gained be changing the columns to perform indirect splits instead of direct splits.

Alternative 2: Reactive distillation

The metathesis of 2-pentene is a convenient system for reactive distillation because the reactant is the intermediate boiling component. As reaction proceeds in the column, butene and hexene are formed and readily separated away from the reactive zone. This results in nearly complete conversion of pentene. We will use feasibility analysis to capture reactive distillation design alternatives for this system. A three-step algorithm is developed based on decomposing full columns into sections. First, feasible regions are identified for each column section. Optimization techniques are then used to

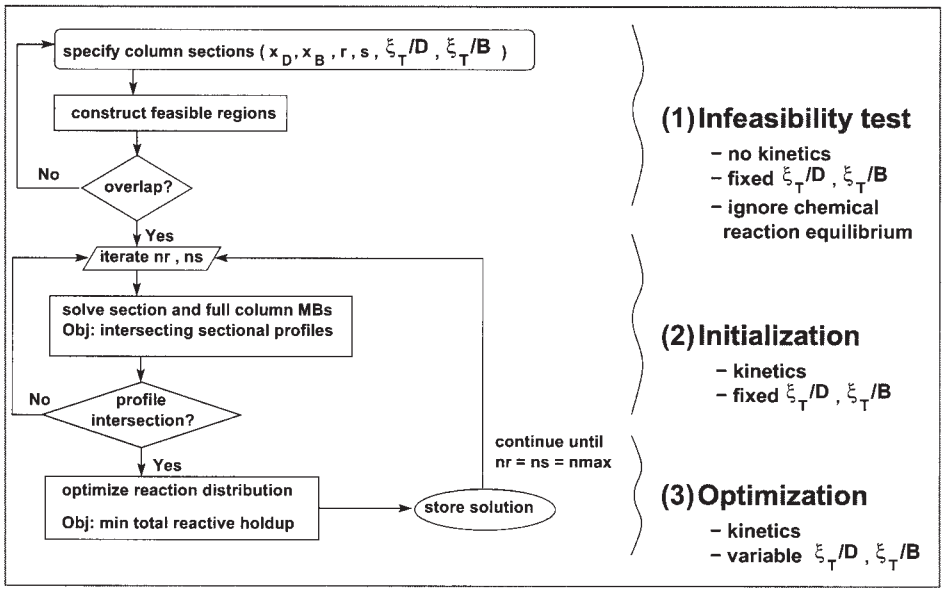

Figure 2. Design algorithm for single-feed reactive distillation columns.

search the regions and connect the sections with the objective of finding a feasible design. The final step optimizes the design in terms of operating parameters. A flowchart illustrating the key steps in the algorithm is presented in Figure 2. Each step will be described in detail as it pertains to the olefin metathesis system.

Initially, we study single-feed reactive distillation columns consisting of two end sections, one rectifying and one stripping, joined by a feed stage. We are able to capture all feasible profiles for both end sections using the feasible regions identified by Hoffmaster and Hauan.[12] These regions are constructed similar to the *bow-tie* approach[15,16] for nonreactive distillation. In brief, the procedure consists of identifying both the reactive and nonreactive pinch points and connecting them with stage-by-stage profiles with extreme policies for internal reaction distribution. There are four types of feasible regions we could use to study this column. One type captures sectional profiles for all possible reaction distribution policies that result in a desired composition, such as distillate or bottoms product. Reaction distribution represents the placement of reaction within a column section and is defined in terms of reaction turnover. Per-stage reaction turnovers are computed from the rate of reaction defined by kinetics and the amount of material reacting defined by the liquid holdup. In this type of feasible region, the external reflux ratio and total amount of reaction are fixed. The region contains sectional profiles for any reaction distribution policy and any number of stages that reach the specified composition.

The metathesis column specifications are given in Table 1. The distillate is 98 mol % butene, whereas the bottoms is 98 mol % hexene. Assuming a pure pentene feed, we determine how much reaction must occur in the full column (ξ_T/F) and the product flow ratio (D/B) using the overall material balance for an isomolar reaction ($\sum \boldsymbol{\nu} = 0$) given by Eq. 2. For this column, the total reaction turnover is $\xi_T/F = 0.49$, and the product flow ratio is $D/B = 1$.

$$z_F = \frac{D/B}{(D/B)+1}\boldsymbol{x}_D + \frac{1}{(D/B)+1}\boldsymbol{x}_B - \frac{\xi_T}{F}\boldsymbol{\nu} \tag{2}$$

To construct the variable distribution feasible regions, we must specify how much reaction occurs in the two end sections. It is not required to place the full amount of reaction in the two sections because additional reaction can occur on the feed stage. Initially, we assume 92% of the total reaction occurs in both end sections, or $\xi_T/D = 0.45$ for the rectifying section and $\xi_T/B = 0.45$ for the stripping section. The remaining 8% occurs on the feed stage. In addition to the reaction turnover specifications, we must set the external reflux and reboil ratios. We initially select $r = 2$ and $s = 3$. Later, these specifications will be relaxed. The energy balance, given by Eq. 3 for an isomolar reaction, relates the reflux, reboil, and feed quality. For the selected reflux and reboil ratio, the feed to the column is a saturated liquid ($q = 1$). The energy balance ensures that the flow rates from the feed stage satisfy the flow balances in both the rectifying and stripping sections.

$$q = \frac{s + 1 - r\cdot(D/B)}{(D/B)+1} \tag{3}$$

Table 1. Specifications for Examples 1 and 2

Example	Specification	Mole Fraction		
1		C_4H_8	C_5H_{10}	C_6H_{12}
	x_D	9.8×10^{-1}	1.995×10^{-2}	5×10^{-5}
	x_B	5×10^{-5}	1.995×10^{-2}	9.8×10^{-1}
	z_F	0	1	0
2		*A*	*B*	*C*
	x_D	9.99×10^{-1}	1×10^{-3}	1×10^{-10}
	x_B	1×10^{-10}	1×10^{-3}	9.99×10^{-1}
	z_{F1}	0	1	0
	z_{F2}	1	0	0

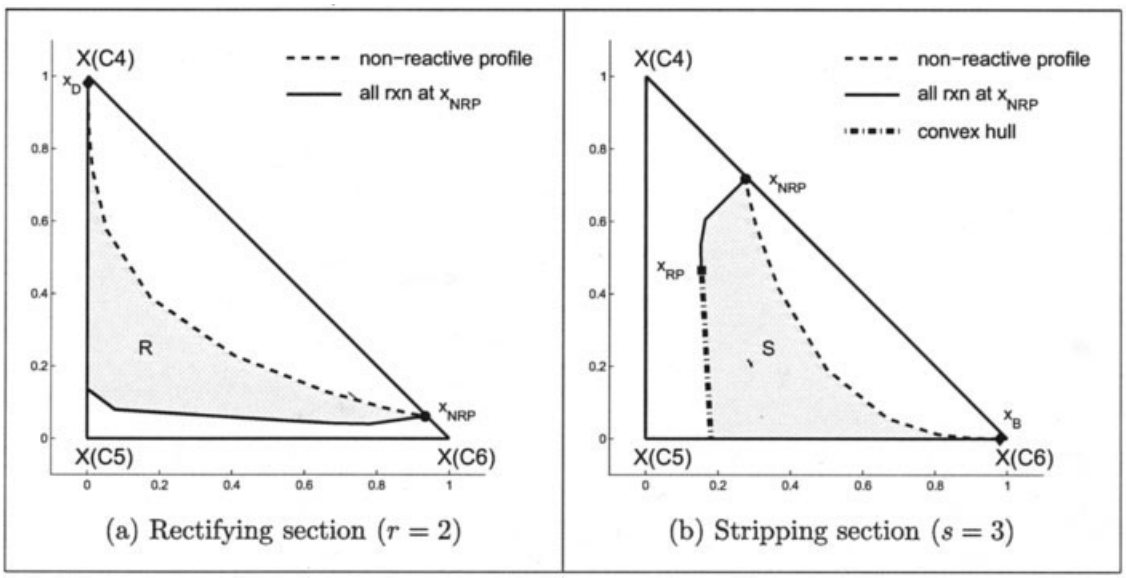

Figure 3. Variable reaction distribution feasible regions for olefin metathesis system.

Figure 3 illustrates the variable reaction distribution feasible regions under these specifications. The rectifying feasible region, shown in Figure 3a, is bounded by the total reaction at the nonreactive pinch and a segment of the butene–pentene binary edge. The bounds on the stripping feasible region in Figure 3b constitute the total reaction at the nonreactive pinch, a convex hull approximation, and a segment of the pentene–hexene edge. These regions neglect kinetics by assuming any fraction of the total reaction in the section may occur on any stage. As a result of this assumption, the feasible regions overestimate the true feasible space and can be used to test only for infeasibility. If Figures 3a and 3b are overlaid, the feasible regions intersect in composition space, which indicates that the column section specifications are potentially feasible, meaning that a design may exist to simultaneously produce the two desired products from a single-feed column.[12] If the regions do not intersect, the infeasible specifications need to be adjusted until overlapping feasible regions are found. Note that the test for overlapping regions becomes a challenging task as the number of components increases beyond three and thus requires the intersection of (hyper)volumes. Herein, we deal with ternary systems only and feasibility may be assessed using planar intersection of the line segments along the feasible region boundaries.

Once a potentially feasible set of specifications is identified, the next step of the algorithm in Figure 2 is to search the regions for feasible designs. In this step, the objective is to identify a feasible design using kinetics to determine per-stage reaction turnovers. When searching the column section regions, several criteria must be met for full-column feasibility. First of all, the rectifying and stripping section profiles must satisfy the stage-to-stage material balance equations for their respective sections. Each section must also achieve the total turnover specification when kinetics and per-stage liquid holdups are used to compute the amount of reaction on each stage. Hoffmaster[17] summarizes the rectifying and stripping section equations formulated in terms of difference points[18] and dimensionless parameters.[19] There are also several constraints necessary to satisfy the full-column material balance and connecting the column sections. To satisfy the overall column balance, the remaining amount of reaction that did not occur in the two sections must be done on the feed stage. Again, the kinetics determine whether this is possible and what the corresponding holdup would be.

The feed stage serves the purpose of connecting the rectifying and stripping sections and ensuring flow rates and compositions match at the connection. Rectifying stage numbers increase from zero at the condenser to nr at the feed stage. Stripping stage numbers begin with zero for the reboiler and increase to ns at the feed stage. The final material balance for the rectifying section is computed around stage $nr - 1$ to determine $\boldsymbol{y}_{nr}$. A phase equilibrium calculation from this composition determines $\boldsymbol{x}_{nr}$, the liquid composition leaving the feed stage. In the stripping section, the final material balance is constructed around stage $ns - 1$ to determine $\boldsymbol{x}_{ns}$. This is also the composition of the liquid leaving the feed stage. To connect the rectifying and stripping sections, the compositions $\boldsymbol{x}_{nr}$ and $\boldsymbol{x}_{ns}$ must match.[20] In composition space, this corresponds to an intersection of the rectifying and stripping section profiles. When the total reaction has taken place and the sectional profiles intersect, the feed stage and full column material balances are satisfied.

Two additional constraints are placed on the column. We assume that only net forward reaction occurs on any stage in the column. This corresponds to the monotonic reaction assumption used in defining the feasible regions. As a result, reaction is not placed on stages with compositions that react in the reverse direction. We also place an upper limit on the amount of reactive liquid holdup on any stage to avoid designs with an unreasonably large liquid holdup. The rationale behind these feasibility constraints are summarized by Hoffmaster.[17] Once feasibility is achieved, we optimize the design in terms of reaction distribution to minimize the total liquid holdup in the column. The models for the rectifying section, stripping section, feed stage, and full column are formulated as nonlinear

programs (NLPs). The feasibility and optimization algorithm proceeds as follows:

Step 1. Specify Number of Stages in Each Column Section. The number of stages in the rectifying and stripping sections are initialized with $nr = 2$ and $ns = 2$. This corresponds to a full column with a condenser, reboiler, one rectifying stage, one stripping stage, and a feed stage.

Step 2. Initialize Rectifying and Stripping Sections. As shown in Eq. 4, the rectifying section is initialized by solving the material balance equations with an objective of minimizing the total liquid holdup in the section. The Damköhler number (Da_n) represents a dimensionless amount of reactive liquid holdup on stage n.[19] Hoffmaster[17] explains why the Damköhler number is convenient for capturing per-stage reactive liquid holdups. This initialization technique results in a rectifying sectional profile that achieves ξ_T/D, the specified amount of reaction for the rectifying section. A similar approach is used to initialize the stripping section as shown in Eq. 5. Similar initialization schemes have been shown to improve the convergence of full-column models.[21]

$$\min \frac{k_{f,\mathrm{ref}}}{D} \sum_{i=0}^{nr-1} H_i = \sum_{i=0}^{nr-1} \mathrm{Da}_i$$
$$\text{s.t. retifying model}$$
$$\sum_{i=0}^{nr-1} \frac{\xi_i}{D} = \frac{\xi_T}{D} \tag{4}$$

$$\min \frac{k_{f,\mathrm{ref}}}{B} \sum_{j=0}^{ns-1} H_j = \sum_{j=0}^{ns-1} \mathrm{Da}_j$$
$$\text{s.t. stripping model}$$
$$\sum_{j=0}^{ns-1} \frac{\xi_j}{B} = \frac{\xi_T}{B} \tag{5}$$

Step 3. Find a Feasible Full-Column Design. This step applies the full-column equations to find a feasible design. Equation 6 shows the model for finding a feasible full-column design. We use a feasibility objective function similar to Melles et al.[22] but represent stage numbers by integer variables and thus implicitly assume that all external feeds enter the column on a particular stage and not in between them. The objective is formulated as minimizing the distance between the final liquid composition on the rectifying and stripping profiles. This objective minimizes the infeasibility in the initial design and seeks to find near feasible starting points. Each section must satisfy the specified amount of reaction for the respective section. In addition, the full column, including the feed stage, must have a total turnover of ξ_T/F. Because the amount of reaction in each section is scaled by the product flow rate, which may differ between sections, we rescale them in terms of the feed flow rate so they can be added together.

$$\min \sqrt{\sum (\boldsymbol{x}_{nr} - \boldsymbol{x}_{ns})^2}$$
$$\text{s.t. full model}$$
$$\sum_{i=0}^{nr-1} \frac{\xi_i}{D} = \frac{\xi_T}{D}$$
$$\sum_{j=0}^{ns-1} \frac{\xi_j}{B} = \frac{\xi_T}{B}$$
$$\frac{D/B}{(D/B)+1} \sum_{i=0}^{nr-1} \frac{\xi_i}{D} + \frac{1}{(D/B)+1} \sum_{j=0}^{ns-1} \frac{\xi_j}{B} + \frac{\xi_f}{F} = \frac{\xi_T}{F} \tag{6}$$

Step 4. If Feasible, Optimize the Design. A design is considered feasible if $\sqrt{\sum (\boldsymbol{x}_{nr} - \boldsymbol{x}_{ns})^2} \le \varepsilon$, where ε is very small: 1×10^{-8}. When the result of Step 3 satisfies this criterion, we use this condition as a constraint and optimize the design in terms of reaction distribution using Eq. 7. We release the constraints that force a certain amount of reaction to take place in each section and allow the reaction to occur anywhere in the full column. The objective is to minimize the total amount of reactive liquid holdup in the column. The advantage of finding a feasible design before performing the optimization is that the solution to the optimization can at worst be the same as the initially feasible design:

$$\min \frac{k_{f,\mathrm{ref}}}{F} H_T = \mathrm{Da}_T$$
$$\text{s.t. full model}$$
$$\sqrt{\sum (\boldsymbol{x}_{nr} - \boldsymbol{x}_{ns})^2} \le \varepsilon$$
$$\frac{D/B}{(D/B)+1} \sum_{i=0}^{nr-1} \frac{\xi_i}{D} + \frac{1}{(D/B)+1} \sum_{j=0}^{ns-1} \frac{\xi_j}{B} + \frac{\xi_f}{F} = \frac{\xi_T}{F} \tag{7}$$

Step 5. Increment the Number of Stages by One and Go to Step 2. If a solution is found, the results are stored. Then we increment the number of rectifying and stripping stages and return to Step 2. For each combination of *nr* and *ns*, we search for feasible and then locally optimal designs. An average of 15 s is necessary* to perform the initialization and optimization for each *nr–ns* combination. When an upper limit on the number of stages in each section (*nmax*) is reached, the algorithm terminates. Each stored design has a locally optimal reaction distribution policy.

We apply this algorithm with a heuristically chosen, system-specific value of $nmax = 15$ to search the feasible regions in Figure 3. Step 3 of the algorithm finds feasible single-feed designs under the conditions used to construct the regions. These designs are then optimized in terms of holdup distribution. Figure 4a illustrates all the locally optimal designs obtained at $r = 2$ and $s = 3$. The trade-off curve, indicated by the solid line, represents the designs with the least amount of total holdup for a given number of stages. A schematic of the "best" design with 20 stages is shown in Figure 4b. The design has a total holdup of $\mathrm{Da}_T = 4.49$ with the majority of the reaction occurring in the middle of the column. We also repeated the entire algorithm for reflux ratios in the range $r \in [1, 6]$ with the same $\boldsymbol{x}_D$, $\boldsymbol{x}_B$, $\boldsymbol{z}_F$, and q. These designs are shown in Figure 5.

* Designs are computed using GAMS and Conopt2 on AMD Athlon 1700+ with 512-MB RAM.

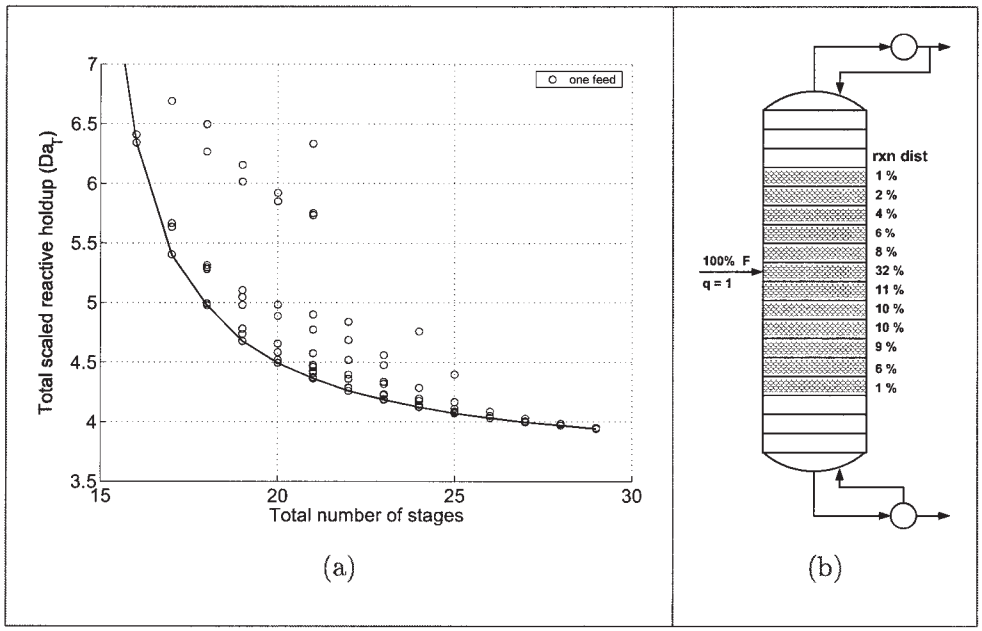

Figure 4. Single-feed olefin metathesis designs with fixed external reflux ratio ($r = 2$) and external reboil ratio ($s = 3$).

(a) Trade-off curve; (b) best 20 stage design ($Da_T = 4.49$).

Each trade-off curve shows the relationship between holdup and reflux for a fixed number of stages. A lower reflux can be used as more stages are added, but the holdup increases substantially. There is also an optimum reflux that results in the least holdup for a given number of stages. For comparison, Okasinski and Doherty[6] present a feasible design under the same conditions with 13.3 stages and a constant per-stage holdup of Da = 0.5, or $Da_T = 6.65$, at $r = 4$. This design is indicated in Figure 5 with an asterisk. By optimizing the reaction distribution policy, the amount of holdup can be reduced by 13% to $Da_T = 5.77$ with 13 stages. For 25 stages and $r = 2$, the holdup can be reduced by 39% to $Da_T = 4.06$. Before selecting an optimal design, these trade-off curves should be translated into economics to determine the optimal combination of reflux, number of trays, and holdup.

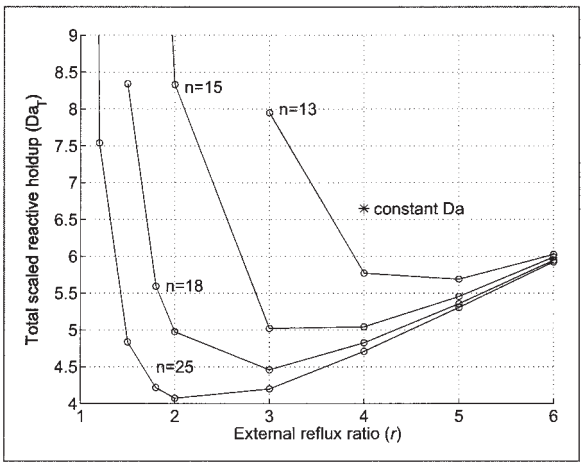

Figure 5. Single-feed olefin metathesis designs for $r \in [1, 6]$ and $q = 1$.

To further improve these designs, we reformulate the material balance equations to account for reactive column sections with multiple feeds. The equations are given in Hoffmaster and Hauan.[12] The feed to the column may be distributed over any number of stages excluding the condenser and reboiler. Each feed stream has the same composition, but we allow the quality of each stream to vary. The algorithm for the single-feed case is used to first find a feasible design. Then the multifeed material balance equations are incorporated into Step 4 to simultaneously optimize feed and reaction distribution. Constraints are added to ensure that the necessary amount of feed enters the column and that the vapor and liquid flow rates match at the intersection of the rectifying and stripping sections. We no longer require any feed to enter on the intersecting stage. In Figure 6a, we show the trade-off curves for multifeed designs with feeds of different qualities. Each trade-off curve has designs with feeds over a particular range of feed qualities. All of the designs have the same external reflux ratio, external reboil ratio, distillate product, and bottoms product as used in Figure 4a. The designs show improvement as the feed quality varies over a larger range. The "best" design with 20 stages is shown in Figure 6b. This design uses two feed stages, and the holdup is reduced by 11% to $Da_T = 4.02$ compared to the single-feed design in Figure 4b. The subcooled liquid feed from above and superheated vapor feed from below result in large flow rates in the middle of the column and high reaction turnovers for the middle stages. Although the designs show significant improvement as the feed quality range expands outside the saturated regime, an economic study is necessary to determine whether it is cost effective to subcool and superheat the feeds. The important result to take from these studies is that feed quality effects should be considered in the design of reactive distillation columns. However, the range of reasonable feed qualities must be carefully determined.

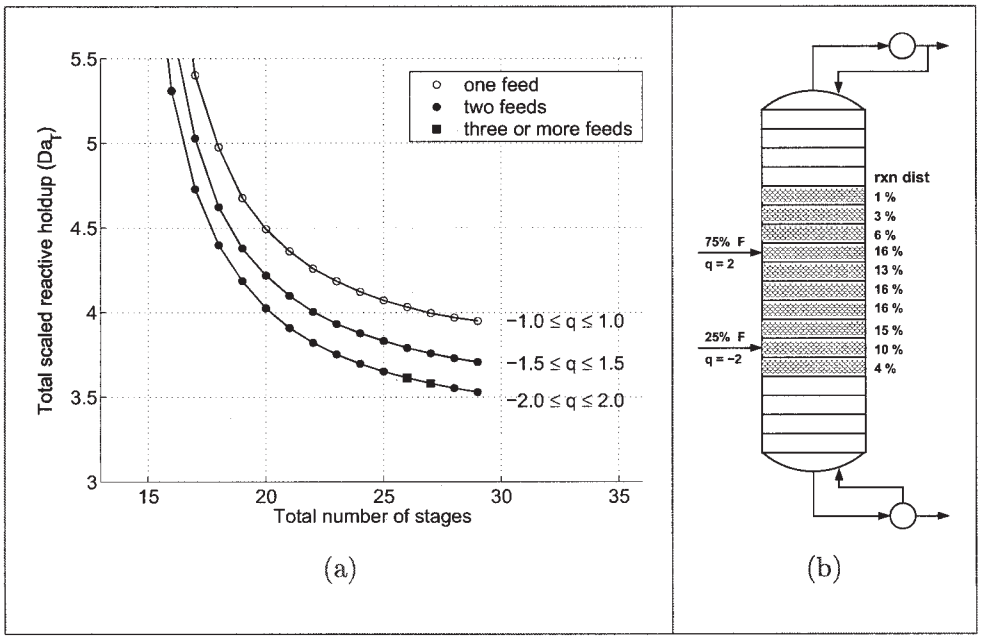

Figure 6. Multifeed olefin metathesis designs with fixed external reflux ratio ($r = 2$), fixed external reboil ratio ($s = 3$), and variable-feed quality.

(a) Trade-off curves; (b) best 20 stage design ($Da_T = 4.02$).

Example 2: Constant relative volatility mixture

The next example investigates how to find a feasible multifeed reactive distillation column design using the concept of limit lines.[12] We select a mixture of components A, B, and C with constant relative volatilities of $\alpha_{AC} = 6$ and $\alpha_{BC} = 3$. The mixture reacts as $A + B \rightarrow 2C$. For this system, one possible column configuration has the heavier feed (F1) entering above the reactive zone and the lighter feed (F2) entering below. We seek out a design with this configuration that feeds component B as F1 and an excess of component A as F2 to produce a bottoms product of component C with 99.9 mol % purity. The specified compositions in the column are given in Table 1. Both feeds are assumed to be saturated liquids. We also specify the distillate–bottoms flow ratio as $D/B = 0.7$ and determine $F1/D = 0.716$, $F2/D = 1.7126$, and $\xi_T/D = 0.7136$ from the overall material balance. Given these specifications, we will identify where to place the feeds and reactive stages to make the full-column design feasible.

In the uppermost portion of the column, we must determine the stage number for the first feed. This section is a side feed rectifying end section. Two operating parameters, which are reflux and feed distribution, describe side feed section profiles and can be captured in a side feed feasible region. For illustrative purposes, we fix the external reflux ratio at $r = 7$ and construct the side feed feasible region containing sectional profiles for all possible feed distribution policies. This region, shown in Figure 7a, is bounded by the nonreactive profile and a segment of the A–C binary edge. Each composition inside the region corresponds to a liquid composition on a stage of the section. Because the feasible region contains an edge of composition space, only certain compositions inside this region can have all of the first feed placed on a single stage and remain stable, that is, the profiles stay inside the valid composition space. There are other stage compositions that cause the profile to become unstable if the feed is added. A minimum mole fraction of each component exists at which the feed may be added and the profile remains stable. We can identify these mole fractions by constructing the limit lines for $F1/D$ using the techniques described by Hoffmaster and Hauan.[12] The limit lines for each component are defined as

$$x_{n,i}^{F1} \geq \frac{z_{F1,i}\dfrac{F1}{D} - x_{D,i}}{r + q_{F1}\dfrac{F1}{D}} \tag{8}$$

The resulting limit lines are $x_{n,A}^{F1} \geq -0.1295$, $x_{n,B}^{F1} \geq 0.0927$, and $x_{n,C}^{F1} \geq 0$. The only line that limits the feed placement is the $x_{n,B}^{F1}$ line. It is shown in Figure 7a as $F1/D$. All compositions inside the feasible region that lie to the left of this line can have all of F1 placed on a single stage. Before selecting the stage for the first feed, we need to investigate where reaction and the second feed can occur. Assuming that F1 enters the column above the reactive zone, we can construct another set of limit lines to determine where all reactions can occur in composition space. The limit lines are found by incorporating the reaction term into Eq. 8 to obtain

$$x_{n,i}^{\xi_T} \geq \frac{z_{F1,i}\dfrac{F1}{D} - x_{D,i} + \nu_i\dfrac{\xi_T}{D}}{r + q_{F1}\dfrac{F1}{D}} \tag{9}$$

The constraining limit lines for the reactive zone are $x_{n,B}^{\xi_T} \geq 2 \times 10^{-4}$ and $x_{n,C}^{\xi_T} \geq 0.185$. Because the $x_{n,B}^{\xi_T}$ line lies very

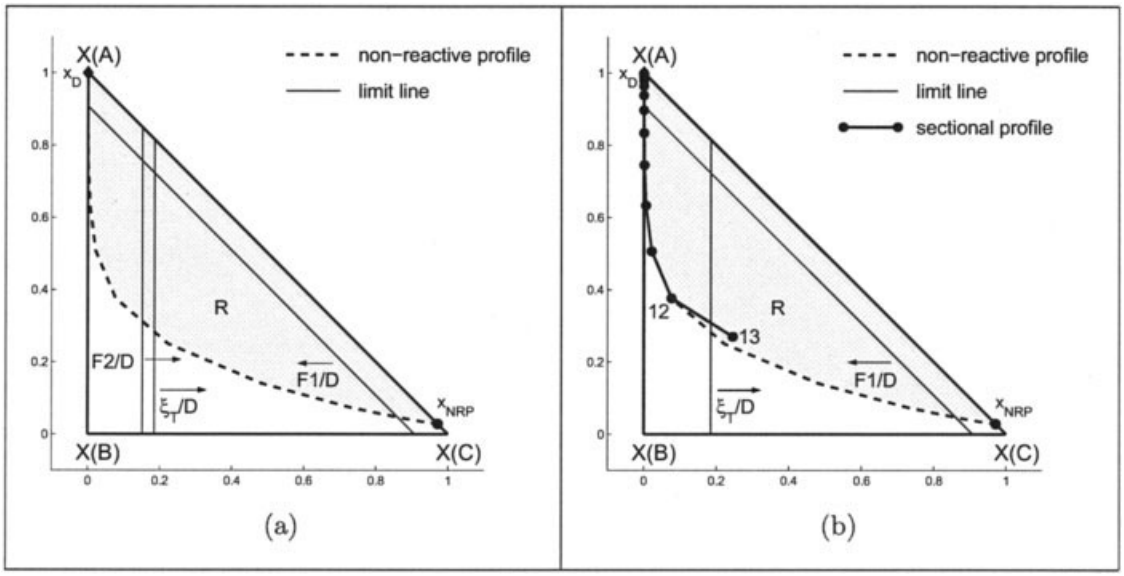

Figure 7. Side feed rectifying end section with a total feed of *F*1/*D* and *r* = 7 using constant volatility mixture.

(a) Variable feed distribution feasible region; (b) side feed section profile with F1 on stage 12.

close to the binary edge, it has little impact on where reaction is placed. The only significant reaction limit line is the $x_{n,C}^{\xi_T}$ line shown in Figure 7a as ξ_T/D. If the total reaction is going to occur on a single stage, it must be placed at a composition to the right of this line. For a reaction distributed over multiple stages, the final stage in the reactive zone must lie to the right of this limit line to keep the profile inside the valid composition space. The final section of the column is a side feed section with the second feed. The limit lines for F2 are given by

$$x_{n,i}^{F2} \geq \frac{z_{F1,i}\dfrac{F1}{D} + z_{F2,i}\dfrac{F2}{D} - x_{D,i} + \nu_i \dfrac{\xi_T}{D}}{r + q_{F1}\dfrac{F1}{D} + q_{F2}\dfrac{F2}{D}} \tag{10}$$

The limit lines for the second side feed are $x_{n,A}^{F2} \geq 0$, $x_{n,B}^{F2} \geq 1 \times 10^{-4}$, and $x_{n,C}^{F2} \geq 0.1514$. Only the $x_{n,C}^{F2}$ line has a significant effect on where the second feed is placed. This line is also shown in Figure 7a as $F2/D$. The second feed must lie to the right of this line.

Given the limit lines for the two side feeds and the reactive zone, we can now choose the stage for the first side feed. We want the next composition after the F1 feed stage to lie to the right of the reaction limit line so the reaction can occur. The first stage that meets this criterion is stage 12. The profile for the side feed rectifying section with the first feed entering on stage 12 is shown in Figure 7b. Next, we construct the feasible region for an internal reactive rectifying section to represent the reactive zone. The region, shown in Figure 8, is bounded by a convex hull approximation because no reactive pinch point is present in the composition interior. All reaction distribution policies move the profile toward the bottoms product. This is convenient because we just need a policy that keeps the next stage after the reactive zone to the right of the F2 limit line. This way the second feed is feasible. Although many options are possible, we arbitrarily choose to do half the reaction on stages 13 and 14. The profile for this policy is shown in Figure 8.

The third and final section of the column is a side feed section. We know the profile is already on the feasible side of the F2 limit line after the reactive zone. However, we need to choose the stage for the second feed so it reaches the necessary bottoms product. This task is simple because after the second feed enters the column the difference point moves exactly to the bottoms product composition. This is a result of choosing

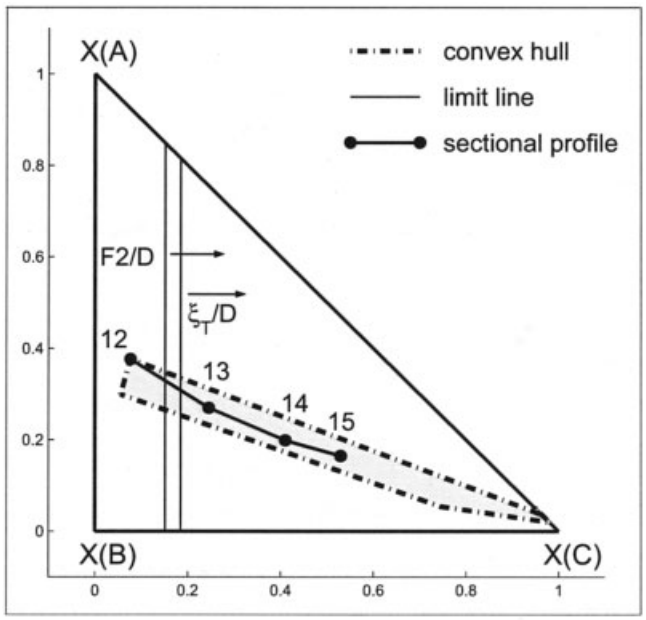

Figure 8. Variable reaction distribution feasible region for reactive internal rectifying section with ξ_T/D using constant volatility mixture.

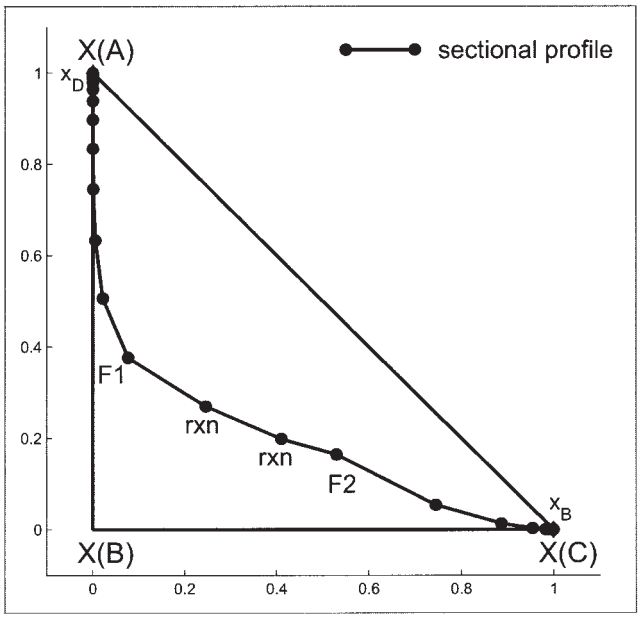

Figure 9. Feasible full column profile for constant volatility mixture.

feed and reaction amounts that satisfy the overall material balance. We select stage 15 for the second feed. When the profile continues from the F2 feed stage, it moves toward the bottoms product. At stage 23, the profile reaches $\boldsymbol{x}_B$. Feasible locations for F2 could also be determined by constructing an internal rectifying side feed feasible region following the reactive zone. For feasibility, the internal region must reach the bottoms product. Feasibility can also be verified for the second feed by constructing a side feed end section feasible region from the bottoms product. The end region must reach the F2 feed stage for feasibility. The feasible full column profile is shown in Figure 9.

Conclusions

We have presented examples illustrating complex column design using feasible regions. For the ideal olefin metathesis system, we used the regions to identify a potentially feasible set of reactive distillation design specifications that were passed to an optimization routine to search the regions for actual designs. Once a feasible design was found, we optimized the design in terms of feed and reaction distribution. Trade-off curves were generated to compare different design alternatives. In the second example, we looked at a constant volatility mixture requiring a multifeed reactive column consisting of side feed and reactive sections. Through the construction of feasible regions and the associated limit lines, we identified feasible locations in the column for the two feeds and the reactive stages. Through these examples, we have shown that regional feasibility analysis of reactive separation cascades is a powerful tool for designing and optimizing complex columns.

Notation

B = bottom product flow rate, amount/time
D = distillate product flow rate, amount/time
Da_n = Damköhler number for stage n
Da_T = total Damköhler number for full column
F = feed flow rate, amount/time
H_n = liquid holdup on stage n, amount
SD = side draw flow rate, amount/time
SF = side feed flow rate, amount/time
T_n = temperature on stage n, K
$k_{f,n}$ = forward reaction rate constant on stage n, 1/time
$k_{f,ref}$ = forward reaction rate constant evaluated at a reference temperature, 1/time
q = quality of side feed/draw, moles of saturated liquid formed/removed on the side stream stage per mole of feed/draw
r = external reflux ratio
$(\mathrm{rate})_n$ = composition-dependent part of kinetic expression on stage n
s = external reboil ratio
$x_{n,i}$ = liquid mole fraction of component i on stage n
$y_{n,i}$ = vapor mole fraction of component i on stage n
$z_{n,i}$ = arbitrary phase mole fraction of component i on stage n

Greek letters

$\alpha_{i,j}$ = relative volatility of component i to component j, $\alpha_{i,j} = (y_i/x_i)/(y_j/x_j)$
α_n = internal reflux or reboil ratio on stage n
δ_n = cascade difference point composition for stage n
ν_i = stoichiometric coefficient for component i
ξ_n = reaction turnover on stage n, amount/time
ξ_T = total reaction turnover in column section, amount/time

Subscripts

B = bottom product
D = distillate product
F = feed
NRP = nonreactive pinch point
SD = side draw
SDP = side draw pinch point
SF = side feed
SFP = side feed pinch point

Literature Cited

1. Pyhälahti A. Reactive distillation in literature. Technical report no. 42. *Plant Design Report Series*. Helsinki, Finland: Helsinki University of Technology; August 1996.
2. Taylor R, Krishna R. Modelling reactive distillation. *Chem Eng Sci.* 2000;55:5183-5229.
3. Venkataraman S, Chan WK, Boston JF. Reactive distillation using Aspen Plus. *Chem Eng Prog.* 1990;86:45.
4. Pérez-Cisneros ES, Schenk M, Gani R, Pilavachi PA. Aspects of simulation, design and analysis of reactive distillation systems. *Comp Chem Eng Suppl.* 1996;20:S267-S272.
5. Buzad G, Doherty MF. Design of three-component kinetically controlled reactive distillation columns using fixed-point methods. *Chem Eng Sci.* 1994;49:1947-1963.
6. Okasinski MJ, Doherty MF. Design methods for kinetically controlled, staged reactive distillation columns. *Ind Eng Chem Res.* 1998;37:2821-2834.
7. Giessler S, Danilov RY, Pisarenko RY, Serafimov LA, Hasebe S, Hashimoto I. Feasibility study of reactive distillation using the analysis of the statics. *Ind Eng Chem Res.* 1998;37:4375.
8. Chadda N, Malone MF, Doherty MF. Feasible products for kinetically controlled reactive distillation of ternary mixtures. *AIChE J.* 2000;46:923-936.
9. Gadewar SB, Malone MF, Doherty MF. Feasible region for a countercurrent cascade of vapor–liquid CSTRs. *AIChE J.* 2002;48:800-814.
10. Ciric AR, Gu D. Synthesis of nonequilibrium reactive distillation processes by MINLP optimization. *AIChE J.* 1994;40:1479-1487.
11. Jackson JR, Grossmann IE. A disjunctive programming approach for the optimal design of reactive distillation columns. *Comp Chem Eng.* 2001;25:1661-1673.
12. Hoffmaster WR, Hauan S. Difference points in extractive and reactive cascades. IV—Feasible regions for multisection columns with kinetic reactions and side streams. *Chem Eng Sci.* 2005;60:7075-7090.

13. Schwab P, Breitscheidel B, Oost C, Schulz R, Schulz M. *Preparation of Propene and, If Desired, 1-Butene*. U.S. Patent No. 6 433 240; 2002.
14. Commereuc D, Mikitenko P. *Process for Metathesis of Olefins in the Presence of a Stabilizing Agent of the Catalyst*. U.S. Patent No. 6 437 209; 2002.
15. Van Dongen DB. *Distillation of Azeotropic Mixtures: The Application of Simple-Distillation Theory to Design of Continuous Processes*. PhD Thesis. Amherst, MA: University of Massachusetts; 1983.
16. Westerberg AW, Wahnschafft O. Synthesis of distillation-based separation systems. *Adv Chem Eng.* 1996;23:63-170.
17. Hoffmaster WR. *Feasible Regions for Azeotropic and Reactive Distillation Systems*. PhD Thesis. Pittsburgh, PA: Carnegie Mellon University, 2004.
18. Hauan S, Ciric AR, Westerberg AW, Lien KM. Difference points in extractive and reactive cascades. I—Basic properties and analysis. *Chem Eng Sci.* 2000;55:3145-3159.
19. Hoffmaster WR, Hauan S. Difference points in extractive and reactive cascades. III—Properties of column section profiles with arbitrary reaction distribution. *Chem Eng Sci.* 2004;59:3671-3693.
20. Julka V, Doherty MF. Geometric behaviour and minimum flows for non-ideal multicomponent distillation. *Chem Eng Sci.* 1990;45:1801.
21. Barttfeld M, Aguirre PA. Optimal synthesis of multicomponent zeotropic distillation processes. 1. Preprocessing phase and rigorous optimization for a single unit. *Ind Eng Chem Res.* 2002;41:5298-5307.
22. Melles S, Grievink J, Schrans SM. Optimisation of the conceptual design of reactive distillation columns. *Chem Eng Sci.* 2000;55:2089-2097.

Manuscript received Jun. 19, 2005, and revision received Nov. 30, 2005.